Huber, C., Federolf, P., Nüesch, C., Cattin, P. C., Friederich, N. F., Tscharner, Vinzenz von. (2013). Heel-strike in walking: Assessment of potential sources of intra- and inter-subject variability in the activation patterns of muscles stabilizing the knee joint. Journal of Biomechanic, 46, 1262-1268.

Heel-strike in walking: assessment of potential sources of intra- and inter-subject variability in the activation patterns of muscles stabilizing the knee joint

Cora Huber [1,2], Peter Federolf [3], Corina Nüesch [4], Philippe C. Cattin [5], Niklaus F. Friederich [6], Vinzenz von Tscharner[7]

[1] Laboratory for Biomechanics and Biomaterials, Hannover Medical School, Germany

[2] Biomechanics & Calorimetry Center Basel, University of Basel, Switzerland

[3] Norwegian School of Sport Sciences, Oslo, Norway

[4] Orthopaedic Department, University Hospital of Basel, Switzerland

[5] Medical Image Analysis Center, University of Basel, Switzerland

[6] Department of Orthopaedic Surgery and Traumatology, Kantonsspital Bruderholz, Switzerland

[7] Human Performance Laboratory, University of Calgary, Canada

Submitted as
Original Article
to
Journal of Biomechanics

Word count (Introduction – Acknowledgement): **3290**
Word count abstract: **248**

Keywords: Gait; EMG; time-frequency analysis; principal component analysis; variability

Corresponding Author
Cora Huber [1, 2]
Department of Orthopaedics
Laboratory for Biomechanics and Biomaterials
Hannover Medical School
Anna-von-Borries-Strasse 1-7
30625 Hannover, Germany
Phone: +49 (0)511 5354 626
Fax: +49 (0)511 5354 875
E-Mail: cora.huber@dhh-gruppe.de

1 Introduction

Electromyography (EMG) is frequently used in studies of neuro-muscular motor control. The number of degrees of freedom in the musculoskeletal system allows for a wide variety of possible movements, and thus requires a complex control system. The flexibility of the musculoskeletal system is illustrated by high step-to-step and inter-subject variability in muscle activation patterns (Araujo et al., 2000; Nair et al., 2010; Winter and Yack, 1987), which can be attributed to anatomical, neuro-muscular, and physiological reasons, among others (De Luca, 1997). However, it remains unknown how different sources of variability contribute to the overall variability in the EMG signals. This study employed a principal component analysis (PCA) to assess the characteristics of EMG variability, and tested hypotheses derived from conceptual considerations of potential mechanical sources of EMG variability associated with the heel-strike event in walking.

Even though EMG signals are highly individual, temporal features of processed EMG signals, such as rhythmicity and timing of muscle activation, are common between individuals (Bizzi et al., 2008; Guidetti et al., 1996; Huber et al., 2011; Hug et al., 2010; Stirling et al., 2011). The application of PCA to EMG signals has enabled extraction of information concerning neuro-muscular processes (Astephen Wilson et al., 2011; Ivanenko et al., 2004), the nature of the movement's coordination (Cappellini et al., 2006; Klarner et al., 2010; Sadeghi et al., 2000, von Tscharner, 2002; von Tscharner and Goepfert, 2003a), and mechanical efficiency (Blake and Wakeling, 2012; Blake et al., 2012). In the present study, PCA was applied to EMG waveforms of the period from 200 ms before heel-strike to 200 ms after heel-strike, in level walking.

Within the analyzed movement, the heel-strike event is likely to be an important source of variability. Both foot placement angle (Murray et al., 1970) and the lateral component of the ground reaction force (Giaskas and Baltzpoulos, 1997) show high step-to-

step variability at heel-strike. It appears that the neuro-muscular control system reacts and adjusts to the specific conditions at each heel-strike (Basmajian and De Luca, 1985) (i.e., mechanical sources of variability), and that these reactions are an important source of EMG
76 variability. The fastest mechanisms that could facilitate adjustments to the conditions at heel-strike are reflex circles, with a reaction time of 30-50 ms (Brooks, 1986; Schmidt and Lee, 1999; Williams et al., 2001). Therefore, a characteristic EMG feature indicating such reflex mechanisms would be maximum variability at approximately 30-50 ms after heel-strike
80 (Fig. 1a). Since reactions to the heel-strike event depend on the specific conditions of each walking step, they may be a source of inter-subject and intra-subject EMG variability. Muscle reactions require a low level of neuronal processing (Williams et al., 2001), and therefore, we hypothesize that these reactions are similar between subjects and that the shape of deviations
84 from the mean EMG waveform may be correlated between subjects.

Another source of inter-subject variability could be the pre-activation of muscles before heel-strike (von Tscharner and Goepfert, 2003b). This pre-activation may be modulated by the so-called muscle tuning mechanism described by Nigg and Wakeling (Nigg,
88 2001; Nigg and Wakeling, 2001). They suggested that the impact at heel-strike could cause potentially harmful shockwaves and vibrations within the body's soft tissues if these shockwaves could not be dampened at impact. However, they suggest that the neuro-muscular system "tunes" itself before impact such that the shockwaves are optimally dampened.
92 Therefore, a characteristic EMG feature associated with this mechanism would be a pre-activation present at heel-strike that persists until reaction cycles can attune the muscles to the specific heel-strike event. As soon as the reaction cycles attenuate the system to the specific heel-strike conditions, one would expect a sharp decline in the activation (Fig. 1b). It has been
96 suggested that muscle tuning is highly subject-specific because vibration and dampening properties of the soft tissue packages depend on the mass and geometry (wobbling mass) of

each individual's soft tissue compartments (Boyer and Nigg, 2006; Nigg and Liu, 1999; Pain and Challis, 2004, 2006). Therefore, the specific waveform shape associated with muscle tuning was not expected to correlate between subjects.

In summary, the primary aim of this study was to calculate and compare principal components (PCs) of intra-subject and inter-subject variability in knee muscle EMG waveforms at heel-strike. It was hypothesized that adaptation to the heel-strike event in walking is a major source of variability. Two waveform shapes with distinct characteristic features were proposed, based on conceptual considerations of how the neuro-muscular system might prepare for, or adapt to, the heel-strike event. A secondary aim was to determine if the calculated PCA waveforms showed the predicted characteristic features of the proposed waveforms.

2 Materials and Methods

2.1 Participants

The study group consisted of ten healthy female volunteers (age: 48 ± 7 years, body mass: 61.1 ± 4.9 kg, height: 1.64 ± 0.05 m [mean ± SD]) with no history of lower extremity surgery, no osteoarthritis of the hip, knee or ankle joints, and no neurological or musculoskeletal impairments. Volunteers were informed about the measurement procedure and provided written consent prior to participation. The local ethics committee approved the study.

2.2 Experimental design

The study protocol consisted of an instrumented three-dimensional gait analysis with synchronous measurement of thigh muscle activity during level walking. A six-camera,

240 Hz motion capture system (Vicon MX13+, Oxford, UK) recorded the positions of retro-reflective markers according to the Vicon Plug-In Gait model (kinematic model V 2.0, Vicon Motion Systems, Oxford, UK; Kadaba et al., 1990). The subjects walked barefoot at a comfortable, self-selected walking speed along a 10 m walkway (1.22 ± 0.06 m/s [mean ± SD]).

2.3 EMG data recording

Surface EMG signals of three quadriceps femoris muscles: rectus femoris (RF), vastus medialis (VM), and vastus lateralis (VL); and two hamstring muscles: semitendinosus (ST) and long head of biceps femoris (BF) were recorded from the left thigh with bipolar Ag/AgCl surface electrodes (diameter: 10 mm, inter-electrode distance: 22 mm, Noraxon U.S.A Inc., Scottsdale, AZ, USA), in accordance with the SENIAM guidelines (Hermens et al., 2000). The ground electrode was positioned over the tibial tuberosity. The electrodes were connected to single differential amplifiers (Biovision, Wehrheim, Germany. Bandwidth 10-700 Hz, gain range 1000-5000). Elastic net bandages (Elastofix, Typ B-25 m stretched, BSN medical GmbH & Co. KG, Hamburg, Germany) were pulled over the thigh to keep cables, amplifiers, and electrodes in place. The EMG data were sampled at 2400 Hz without further processing.

2.4 Data processing

A time-frequency analysis, consisting of 13 non-linearly scaled wavelets (von Tscharner, 2000), yielded time and frequency distributions of the power of the EMG signal. The EMG power at each time frame was defined as the sum of the powers extracted from the wavelets with centre frequencies from 19 to 395 Hz. Wavelets with center frequencies lower than 19 Hz or higher than 395 Hz were omitted from the analysis, as they are known to be highly influenced by movement artifacts (Conforto et al., 1999) and high frequency noise (e.g., 400 Hz power supplies), respectively. EMG power was analyzed from 200 ms before heel-strike to 200 ms after heel-strike, henceforth referred to as a waveform. Each waveform

was represented by 960 data points (sample frequency of 2400 Hz). Time 0 within the waveform was defined to be at heel-strike, which was determined from the vertical position of the heel marker. All waveforms were normalized by the integrated power; thus, the integrated power of the normalized waveforms was always 1. Due to this normalization, information about the degree of muscle activity is lost. Thus, the waveform shapes can be compared between subjects, but the amplitudes cannot. For each subject, 18 waveforms from the left leg were extracted, yielding a total of 180 waveforms available for further processing. Individual mean waveforms were calculated for each muscle by averaging the 18 waveforms of each subject. Group mean waveforms were computed for each muscle by averaging the 10 individual mean waveforms.

The waveforms were stored in an N x p matrix, where N and p represent the number of waveforms and the number of data points in the waveforms, respectively. This matrix was denoted the input matrix (i.e., input matrix to the PCA), and the N waveforms were treated as vectors of a p-dimensional vector space. Two PCA procedures (Jolliffe, 2002), with differing types of input matrices, were performed. In both PCA calculations, the mean waveform of the input matrix was subtracted prior to calculation of the covariance matrix. In the "intra-subject PCA", the individual waveforms of each muscle and subject were assembled into an input matrix M_{18x960}. A total of 50 intra-subject PCAs – one for each subject and muscle – were used to identify correlated deviations from the individual mean activation waveform of a given muscle (intra-subject variability). In addition, an "inter-subject PCA" was performed, by forming an input matrix $M_{180x960}$ from all 180 waveforms of a given muscle (10 subjects x 18 waveforms).

The PCA yielded: (i) the eigenvectors of the covariance matrix of the input matrix, known as principal component vectors; (ii) the eigenvalues; and (iii) the loading factors, known as PC-scores (also known as PC-coefficients or weight factors). The PC-vectors represented correlated deviations from the mean waveform; that is, depending on which PCA

172 procedure was applied, they represented deviations from the individual mean waveform (intra-subject PCA) or from the group mean waveform (inter-subject PCA). The eigenvalues quantified the amount of variance explained by the corresponding PC. In this study, the eigenvalues were normalized by expressing them as a percentage of the sum of all 176 eigenvalues, i.e., as a percentage of the entire variability in the input matrix. The PC-scores were obtained by projecting each waveform onto the PC-vectors. PC-scores are a measure of how similar the measured waveforms are to a specific PC. The group mean waveforms, together with the lower-order PCs, captured the main features and modulations that are 180 common within the analyzed group of waveforms. The higher-order PCs represented fluctuations that were small in amplitude and/or not representative of the whole group.

As a similarity criterion, absolute values of the Pearson's correlation coefficient *r* were calculated for the 10 sets of intra-subject PC-vectors paired with the inter-subject PC-vectors 184 for each of the five muscles.

All analyses were performed in Matlab (The MathWorks, Version R2011a, Natick, MA, USA) using custom-written programs.

188 **3 Results**

A visual representation of the inter-subject and intra-subject variability is shown in Fig. 2. The normalized eigenvalues of the first seven PCs for the inter-subject (Fig. 3, left) and intra-subject (Fig. 3, right) analyses identify two important results. Firstly, a substantial 192 fraction of the EMG waveform variability was represented by only a few PCs. Across all five muscles, the first three inter-subject PCs accounted for 51.8 to 67.9% of the waveform variance, and the first three intra-subject PCs accounted for 63.6 ± 3.9% to 77.7 ± 3.7% (mean ± SD across the five muscles) of the waveform variance. Thus, the individual

196 waveforms reconstructed from the group mean waveform and the first three inter-subject PC-vectors weighted by the mean individual PC-scores (mean over the 18 PC-scores of a subject) (Fig. 2, dashed line) contain enough information to mirror the basic activation pattern of an individual mean waveform (Fig. 2).

200 The second result was that the normalized eigenvalues of the intra-subject analysis agreed with those of the inter-subject analysis: PC_2-eigenvalue range: 17.1-22.9% vs. 19.2 ± 2.0% to 23.7 ± 4.8% (all comparisons: inter vs. intra [mean ± SD] across the five muscles), PC_3: 9.8-12.8% vs. 12.3 ± 2.8% to 14.4 ± 2.6%, PC_4: 8.2-9.5% vs. 7.7 ± 2.0% to
204 9.9 ± 2.2%, PC_5: 5.0-7.3% vs. 5.0 ± 2.0% to 6.5 ± 2.7% PC_6: 4.3-6.2% vs. 3.5 ± 1.5% to 4.3 ± 1.6%. The inter-subject analysis assessed the variability over 180 waveforms – with 10 times more potential sources of variability than the intra-subject analysis. The normalized eigenvalues of the inter-subject analysis might intuitively cover substantially less variability
208 than in the intra-subject analysis. However, a notable increase of the normalized eigenvalues was only displayed in PC_1, for the muscles RF (from 22.2% vs. 32.9 ± 5.6% [all comparisons: inter vs. intra [mean ± SD] across the five muscles]), VM (28.9% vs. 39.0 ± 6.7%), VL (30.2% vs. 37.9 ± 7.1%), and BF (26.1% vs. 32.2 ± 4.3%). The muscle ST showed similar
212 inter-subject and intra-subject variability in PC_1 (39.9% vs. 36.0 ± 5.0%). With regard to PC-vector waveforms, PC_1, displayed a strong correlation between intra-subject and inter-subject analyses, while higher-order PCs displayed moderate correlations (particularly PC_2) or weak/no correlation (PC_3 and higher) (Fig. 4).

216 Based on conceptual considerations, shapes with specific features were predicted (see Introduction) for the correlated deviations from the mean waveform, i.e. the PC-vectors. Such features were found in the first (Fig. 5) and second (Fig. 6) PC-vector. Figure 5 shows for the five analyzed muscles the shape of the inter-subject PC_1-vector (top row) and gives a visual
220 impression of how the waveforms changed when adding the inter-subject PC_1-vectors

weighted with the individual mean PC_1-scores of each subject to the group mean waveform (second row containing 10 graphs). Figure 6 shows the same for PC_2. The main waveform feature predicted for variations in the reaction to heel-strike, an activation peak 30-50 ms after heel-strike, was observed in PC_1 of the muscles VM, VL, ST, and BF (Fig. 5), and in PC_2 of the muscle RF (Fig. 6). These peaks occurred 51.3 ms, 40.0 ms, 52.5 ms, 42.5 ms, and 41.3 ms after heel-strike for the muscles RF, VM, VL, ST, and BF, respectively.

The waveform features that were predicted for variations in the activation prior to heel-strike – high muscle activation after heel-strike followed by a sharp decline at the same time where reactive mechanism peaked – were observed in PC_1 of the muscle RF (Fig. 5) and in PC_2 of the muscles VM, VL, ST, and BF (Fig. 6). All five muscles also showed a gradual increase in muscle activity in these PC-vectors, starting at least 50 ms before heel-strike for the muscles RF, VM, VL and 80-100 ms before heel-strike for the muscles BF and ST. In the three knee extensor muscles (RF, VM, and VL), activation continued to increase after heel-strike, whereas for the knee flexors BF and ST, activation displayed a gradual decline after heel-strike.

The up- or down-regulation of the changes in the waveform as characterized by PC_1 or PC_2 appeared to shift the peak in muscle activation from pre- to post-heel-strike (Figs. 5, 6). The higher-order inter-subject PC-vectors (PC_3 to PC_7) showed multimodal shapes in all muscles with inter-peak time intervals in the range: 53.3 ± 7.8 to 120.8 ± 11.6 ms (Fig. 7).

4 Discussion

This study aimed to assess intra-subject and inter-subject variability of knee muscle EMG signals at heel-strike. The main findings were (i) a large fraction of the variability

(> 60%) was represented using only a few (three) PCs; (ii) the eigenvalues of the second-order and higher-order PCs did not differ between the inter-subject and intra-subject analyses; and (iii) the shapes of the first two PC-vectors agreed well with predicted shapes derived from conceptual considerations.

These findings suggest that the structure within a muscle activation pattern is not randomly organized. A significant fraction of the variability can be explained by a linear combination of distinct activation patterns. The PCA resolved the complex variability in the EMG signal (Fig. 2) into a small number of characteristic waveform deviation patterns (represented by PC-vectors). We hypothesized that these PC-vectors are not mere mathematical constructs, rather that they may be indicative of specific sources of variability affecting the EMG waveform. Specifically, the heel-strike event was identified as a major source of EMG variability, and it was found that for all five analyzed muscles, the shape of the first two PC-vectors exhibited features that had been predicted based on considerations of physiological pre-activation and reaction mechanisms.

Our results suggest that an up- or down-regulation of a reactive mechanism adjusting for the specific conditions present at heel-strike may be an important source of EMG variability represented in the PC_1-vector of the muscles VM, VL, ST, and BF, and in the PC_2-vector of the muscle RF. The strong correlation between inter-subject and intra-subject PC-vectors supports this interpretation. The delay between the heel-strike event and the peak in the PC-vector of the EMG activation was of the same order of magnitude as that previously reported in unconstrained overground walking (af Klint et al., 2010).

Some features associated with pre-activation in preparation for the heel-strike seemed to agree with the shape of the PC_1-vector calculated for the muscle RF and the PC_2-vectors obtained for VM, VL, BF, and ST. Pre-activation ensures that the knee has sufficient stiffness

268 at the moment of heel-strike so as not to collapse; however, in all five muscles, the increase in activation level was only gradual and set in only 50 to 100 ms before heel-strike. Considering that the electromechanical delay between electrical stimulation and force production in a muscle is of the same order of magnitude (Cavanagh and Komi, 1979; Vos et al., 1990; Zhou
272 et al., 1995), it seems questionable that the observed waveform would produce sufficient joint stiffness at the time of heel-strike. However, the observed PC-vector would fit to a mechanical model with variable knee stiffness: still relatively soft at the moment of heel-strike, then rapidly stiffening afterwards. Furthermore, variable knee stiffness due to gradually
276 increasing muscle activation would lead to the soft tissue compartments around the knee vibrating with an increasing rather than a constant frequency. In fact, variable soft-tissue vibration frequencies were recently reported for running by Enders et al. (2012).

Variability in the EMG signal is often interpreted as an indication of different neuronal
280 control strategies (Ranganathan and Krishnan, 2012). However, if our interpretation is correct, a significant fraction of the EMG variability around the time of heel-strike can be attributed to processes that the neuro-muscular system uses to adjust for the mechanical conditions present. Moreover, our results suggest the possibility of distinguishing and
284 separately investigating feedback and feed-forward mechanisms in the EMG signals of complex movements.

Some of the higher-order PC-vectors may be modulations of the two predicted waveforms as they also showed extreme values at approximately 30-50 ms after heel-strike.
288 Other waveforms exhibited a rhythmical variation with two or three oscillations. Recent studies have reported a heel-strike adjusted rhythm in the EMG signal at around 40 Hz in both running (Stirling et al., 2011) and walking (Huber et al., 2011). However, the exact pulse frequency differed between subjects, which might have led to an inter-subject EMG
292 variability that contributed to the higher-order PC-vector waveforms.

This study offers a new approach for analysis and interpretation of the inter-subject and intra-subject variability in the EMG signals of muscles that control the knee joint.Our interpretation is consistent with the present study's results; however, it is not necessarily the only possible interpretation. Further work is necessary to support or contradict these findings, such as an investigation of EMG variability when the heel-strike characteristics are systematically modified.

Conflict of interest statement

The authors report no potential conflict of interest associated with the study presented in this manuscript.

Acknowledgement

The authors would like to thank the Laboratory for Movement Analysis of the Children's University Hospital Basel and the Department of Orthopaedic Surgery of the University Hospital of Basel for their gait analysis equipment. We also acknowledge the financial support of the Emilia Guggenheim-Schnurr foundation, the ProMotio foundation for biomechanical research Basel, and the donation of Dr. med. h.c. H.J. Wyss to the University of Basel in 2004. The authors also thank Beat Göpfert for his technical support and Dr. Tomas Correa for editing English style and grammar.

References

af Klint, R., Cronin, N.J., Ishikawa, M., Sinkjaer, T., Grey, M.J., 2010. Afferent Contribution to Locomotor Muscle Activity During Unconstrained Overground Human Walking: An Analysis of Triceps Surae Muscle Fascicles. Journal of Neurophysiology 103 (3), 1262-1274.

Araujo, R.C., Duarte, M., Amadio, A.C., 2000. On the inter- and intra-subject variability of the electromyographic signal in isometric contractions. Electromyography and Clinical Neurophysiology 40 (4), 225-229.

Arsenault, A.B., Winter, D.A., Marteniuk, R.G., (1986). Is there a 'normal' profile of EMG activity in gait? Medical and Biological Engineering and Computing 24 (4), 337-343.

Astephen Wilson, J.L., Deluzio, K.J., Dunbar, M.J., Caldwell, G.E., Hubley-Kozey, C.L., 2011. The association between knee joint biomechanics and neuromuscular control and moderate knee osteoarthritis radiographic and pain severity. Osteoarthritis and Cartilage 19 (2), 186-193.

Basmajian, J.V, De Luca, C.J., 1985. Muscles Alive: Their Functions Revealed by Electromyography, 5th ed. Williams & Wilkins, Baltimore, MD, USA.

Bizzi, E., Cheung, V.C.K., d'Avella, A., Saltiel, P., Tresch, M., 2008. Combining modules for movement. Brain Research Reviews 57 (1), 125-133.

Blake, O.M., Champoux, Y., Wakeling, J.M., 2012. Muscle Coordination Patterns for Efficient Cycling. Medicine and Science in Sports and Exercise 44 (5), 926-938.

Blake, O.M., Wakeling, J.M., 2012. Muscle Coordination During an Outdoor Cycling Time Trial. Medicine and Science in Sports and Exercise 44 (5), 939-948.

Boyer, K.A., Nigg, B.M., 2006. Soft tissue vibrations within one soft tissue compartment. Journal of Biomechanics 39 (4), 645-651.

Brooks, V., 1986. The Neural Basis of Motor Control. Oxford University Press, New York, USA.

Cappellini, G., Ivanenko, Y.P., Poppele, R.E., Lacquaniti F., 2006. Motor Patterns in Human Walking and Running. Journal of Neurophysiology 95 (6), 3426-3437.

Cavanagh, P.R., Komi, P.V., 1979. Electromechanical delay in human skeletal muscle under concentric and eccentric contractions. European Journal of Applied Physiology 42 (3), 159-163.

Conforto, S., D'Alessio, T., Pignatelli, S., 1999. Optimal rejection of movement artefacts from myoelectric signals by means of a wavelet filtering procedure. Journal of Electromyography and Kinesiology 9 (1), 47-57.

De Luca, C.J, 1997. The Use of Surface Electromyography in Biomechanics. Journal of Applied Biomechanics 13 (2), 135-163.

Enders, H., von Tscharner, V., Nigg, B.M., 2012. Analysis of damped tissue vibrations in time-frequency space: a wavelet-based approach. Journal of Biomechanics 45 (16), 2855-2859.

Frigo, C., Crenna, P., 2009. Multichannel SEMG in clinical gait analysis: a review and state-of-the-art. Clinical Biomechanics 24 (3), 236-245.

Giakas, G., Baltzopoulos, V., 1997. Time and frequency domain analysis of ground reaction forces during walking: an investigation of variability and symmetry. Gait and Posture 5(3), 187-197.

Guidetti, L., Rivellini, G., Figura, F., 1996. EMG patterns during running: Intra- and inter-individual variability. Journal of Electromyography and Kinesiology 6 (1), 37-48.

Hermens, H.J., Freriks, B., Disselhorst-Klug, C., Rau, G., 2000. Development of recommendations for SEMG sensors and sensor placement procedures. Journal of Electromyography and Kinesiology 10 (5), 361-374.

Huber, C., Nüesch, C., Göpfert, B., Cattin, P.C., von Tscharner, V., 2011. Muscular timing and inter-muscular coordination in healthy females while walking. Journal of Neuroscience and Methods 201 (1), 27-34.

Hug, F., Turpin, N.A., Couturier, A., Dorel, S., 2010. Consistency of muscle synergies during pedaling across different mechanical constraints. Journal of Neurophysiology 106 (1), 91-103.

Ivanenko, Y.P., Poppele, R.E., Lacquaniti, F., 2004. Five basic muscle activation patterns account for muscle activity during human locomotion. Journal of Physiology 556 (pt 1), 267-282.

Jolliffe, I.T., 2002. Principal Component Analysis. 2nd ed. Springer, New York, USA.

Kadaba, M.P., Ramakrishnan, H.K., Wootten, M.E., 1990. Measurement of lower extremity kinematics during level walking. Journal of Orthopaedic Research 8 (3), 383-392.

Klarner, T., Chan, H.K., Wakeling, J.M., Lam, T., 2010. Patterns of muscle coordination vary with stride frequency during weight assisted treadmill walking. Gait and Posture 31 (3), 360-365.

Murray, M.P., Kory, R.C., Sepic, S., 1970. Walking patterns of normal women. Archives of physical medicine 51 (11), 637-650.

Nair, S.S., French, R.M., Laroche, D., Thomas, E., 2010. The Application of Machine Learning Algorithms to the Analysis of Electromyographic Patterns From Arthritic Patients. IEEE Transactions on Neural Systems and Rehabilitation Engineering 18 (2), 174-184.

Nigg, B.M., 2001. The Role of Impact Forces and Foot Pronation: A new Paradigm. Clinical Journal of Sports Medicine 11 (1), 2-9.

Nigg, B.M., Liu, W., 1999. The effect of muscle stiffness and damping on simulated force peaks during running. Journal of Biomechanics 32 (8), 849-856.

Nigg, B.M., Wakeling, J.M., 2001. Impact Forces and Muscle Tuning: A new Paradigm. Exercise and Sport Sciences Reviews 29 (1), 37-41.

Pain, M.T.G., Challis, J.H., 2006. The influence of soft tissue movement on ground reaction forces, joint torques and joint reaction forces in drop landing. Journal of Biomechanics 39 (1), 119-124.

Pain, M.T.G., Challis, J.H., 2004. Wobbling mass influence on impact ground reaction forces: A simulation model sensitivity analysis. Journal of Applied Biomechanics 20 (3), 309-316.

Ranganathan, R., Krishnan, C., 2012. Extracting synergies in gait: using EMG variability to evaluate control strategies. Journal of Neurophysiology 108 (5), 1537-1544.

Sadeghi, H., Prince, F., Sadeghi, S., Labelle, H., 2000. Principal component analysis of the power developed in the flexion/extension muscles of the hip in able-bodied gait. Medical Engineering & Physics 22 (10), 703-710.

Schmidt, R., Lee, T., 1999. Motor Control and Learning: A Behavioral Emphasis, 3rd ed. Human Kinetics. Champaign, Ill, USA.

Stirling, L.M., von Tscharner, V., Kugler, P., Nigg, B.M., 2011. Piper rhythm in the activation of the gastrocnemius medialis during running. Journal of Electromyography and Kinesiology 21 (1), 178-183.

von Tscharner, V., 2000. Intensity analysis in time-frequency space of surface myoelectric signals by wavelets of specified resolution. Journal of Electromyography and Kinesiology 10 (6), 433-445.

von Tscharner, V., 2002. Time–frequency and principal-component methods for the analysis of EMGs recorded during a mildly fatiguing exercise on a cycle ergometer. Journal of Electromyography and Kinesiology 12 (6), 479-492.

von Tscharner, V., Goepfert, B., 2003a. Gender dependent EMGs of runners resolved by time/frequency and principal component analysis. Journal of Electromyography and Kinesiology 13 (3), 253-272.

von Tscharner, V., Goepfert, B., 2003b. Changes in EMG signals for the muscle tibialis anterior while running barefoot or with shoes resolved by non-linearly scaled wavelets. Journal of Biomechanics 36 (8), 1169-1176.

Vos, E.J., Mullender, M.G., van Ingen Schenau, G.L., 1990. Electromechanical delay in the vastus lateralis muscle during dynamic isometric contractions. European Journal of Applied Physiology and Occupational Physiology 60 (6), 467-471.

Williams, G.N., Chmielewski, T., Rudolph, K.S., Buchanan, T.S., Snyder-Mackler, L., 2001. Dynamic Knee Stability: Current Theory and Implications for Clinicians and Scientists. Journal of Orthopaedic and Sports Physical Therapy 31 (10), 546-566.

Winter, D.A., Yack, H.J., 1987. EMG profiles during normal human walking: stride-to-stride and inter-subject variability. Electroencephalography and Clinical Neurophysiology 67 (5), 402-411.

Zhou, S., Lawson, D.L., Morrison, W.E. Fairweather, I., 1995. Electromechanical delay of knee extensors: the normal range and the effects of age and gender. Journal of Human

Movement Studies 28 (3), 127-146.

Figures

Fig. 1: Predicted components of the EMG waveform derived from conceptual considerations of mechanisms that may play a role in the adaptation to the heel-strike. (a) Variability peak due to attenuation of muscle activity to the specific heel-strike conditions, based on an assumed reaction time of around 30 ms. (b) Pre-activation prior to impact, persisting until the system attenuates to the specific impact conditions. The predicted waveforms (solid lines) are affected by the normalization (in the present study, to unit power) that is necessary for comparison of EMG signals between subjects (De Luca, 1997; Frigo and Crenna, 2009). The dashed lines in (a) and (b) show a possibility of how the waveform might be distorted, taking into account that muscle activation in the analyzed muscles is mostly absent 200 ms before and 200 ms after heel-strike (Arsenault et al, 1986).

Fig. 2. The individual mean waveforms for each of the ten subjects (s01 to s10, solid black lines), and the waveforms reconstructed from the group mean waveform and the first three inter-subject PC-vectors weighted by the individual mean PC-scores (dashed black lines) for the following muscles: rectus femoris, vastus medialis, vastus lateralis, semitendinosus, and biceps femoris. Intra-subject variability is indicated by gray shaded areas representing the standard error of the mean calculated for each subject. Each waveform has been scaled by its maximum range. Time 0 indicates heel-strike (vertical black line).

Fig. 3. The percentage variability explained by the first seven principal components (gray shaded bars) for the inter-subject PCA (left) and the intra-subject PCA (right, error bars

represent SDs across the 10 subjects) for the following muscles: rectus femoris (RF), vastus medialis (VM), vastus lateralis (VL), semitendinosus (ST), and biceps femoris (BF).

Fig. 4. Distributions of the correlation coefficients calculated for the 10 sets of intra-subject PC-vectors paired with the inter-subject PC-vector for the first seven PCs. Negative correlation coefficients have been inverted.

Fig. 5. Shape of the inter-subject PC_1-vector (top row) and line graphs for each of the 10 subjects (s01 to s10) representing changes in the waveform when the PC_1-vector (weighted by the individual mean PC_1-score of each subject) was added to the group mean waveform (second row containing 10 graphs). The waveforms have been sorted from positive to negative PC_1-scores (displayed within each graph). Each waveform has been scaled by its maximum range.

Fig. 6. Shape of the inter-subject PC_2-vector (top row) and line graphs for each of the 10 subjects (s01 to s10) representing changes in the waveform when the PC_2-vector (weighted by the individual mean PC_2-score of each subject) was added to the group mean waveform (second row containing 10 graphs). The waveforms have been sorted from positive to negative PC_2-scores (displayed within each graph). Each line graph is scaled by its maximum range.

Fig. 7. Higher-order inter-subject PC-vectors: PC_3- (first row), PC_4- (second row), PC_5- (third row), PC_6- (fourth row), and PC_7-vectors (sixth row). Time 0 indicates heel-strike (vertical
468 black line).

Fig#1

Click here to download high resolution image

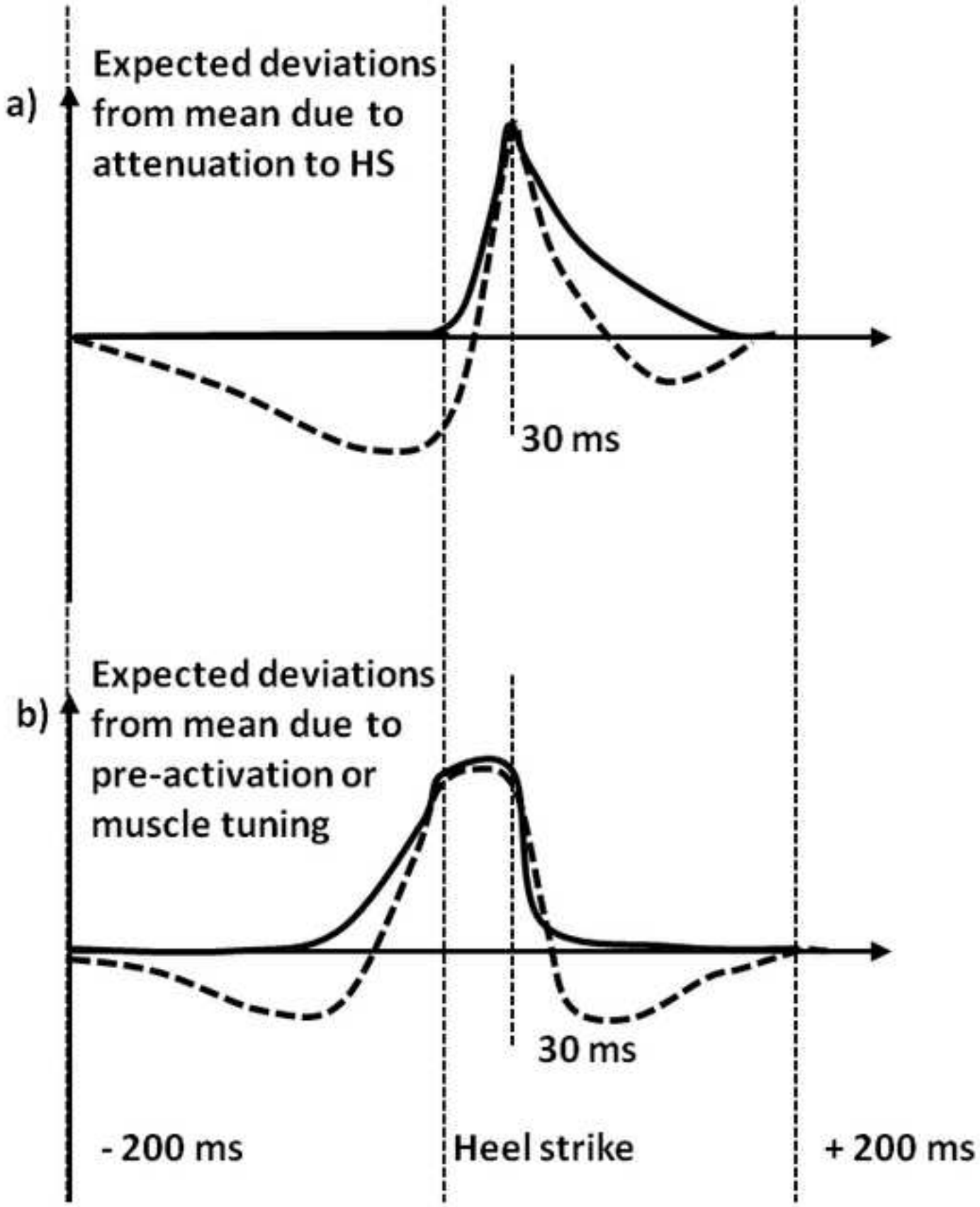

Fig#2

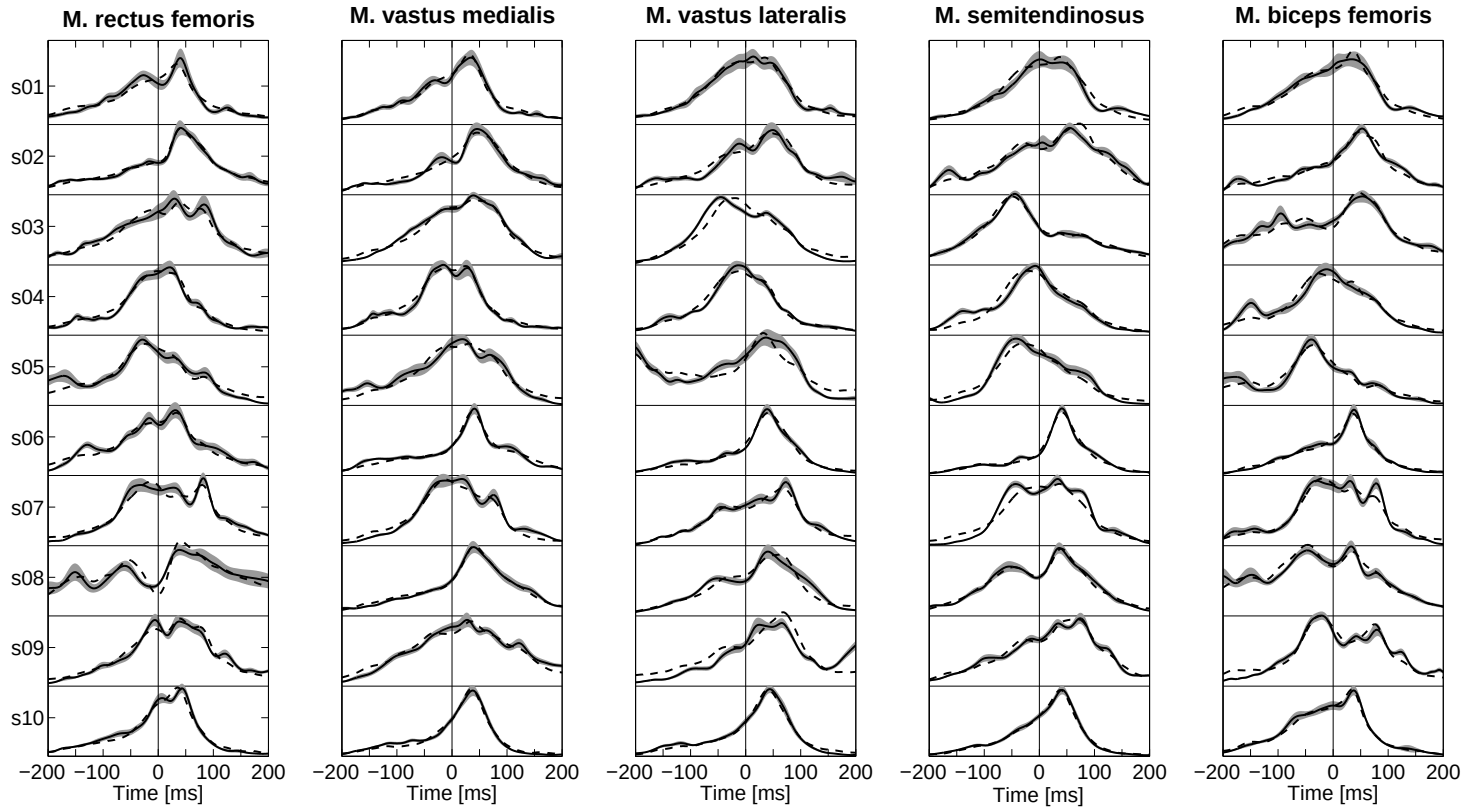
M. rectus femoris
M. vastus medialis
M. vastus lateralis
M. semitendinosus
M. biceps femoris
s01
s02
s03
s04
s05
s06
s07
s08
s09
s10
−200 −100 0 100 200
Time [ms]

Fig#3

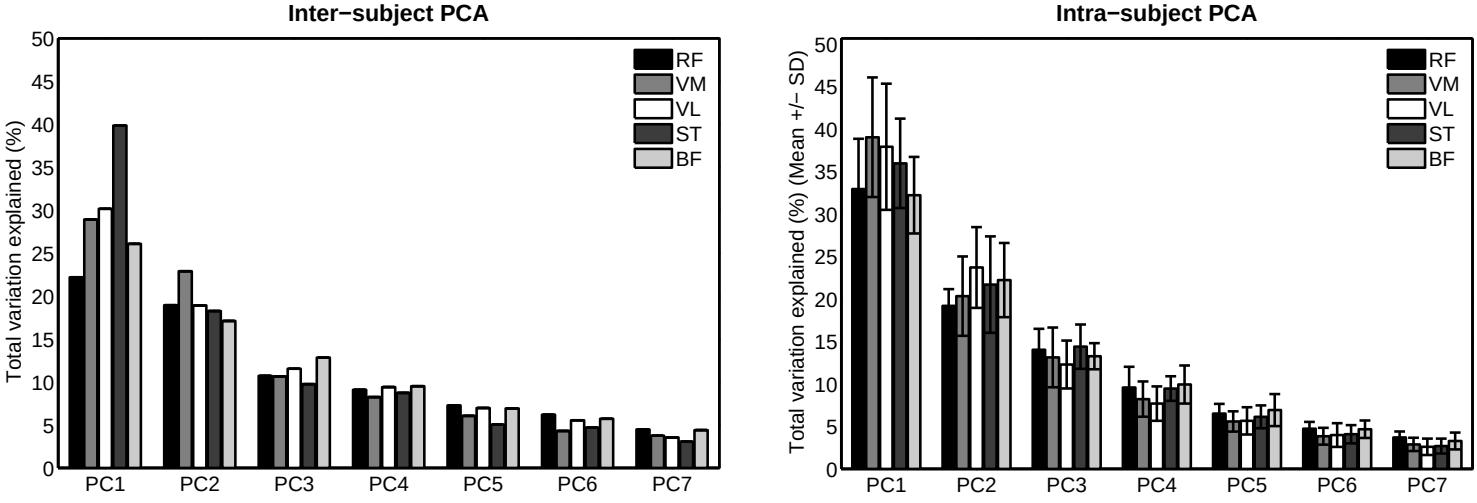
Inter−subject PCA
Total variation explained (%)
0
5
10
15
20
25
30
35
40
45
50
PC1
PC2
PC3
PC4
PC5
PC6
PC7
RF
VM
VL
ST
BF
Intra−subject PCA
Total variation explained (%) (Mean +/− SD)
0
5
10
15
20
25
30
35
40
45
50
PC1
PC2
PC3
PC4
PC5
PC6
PC7
RF
VM
VL
ST
BF

Fig#4

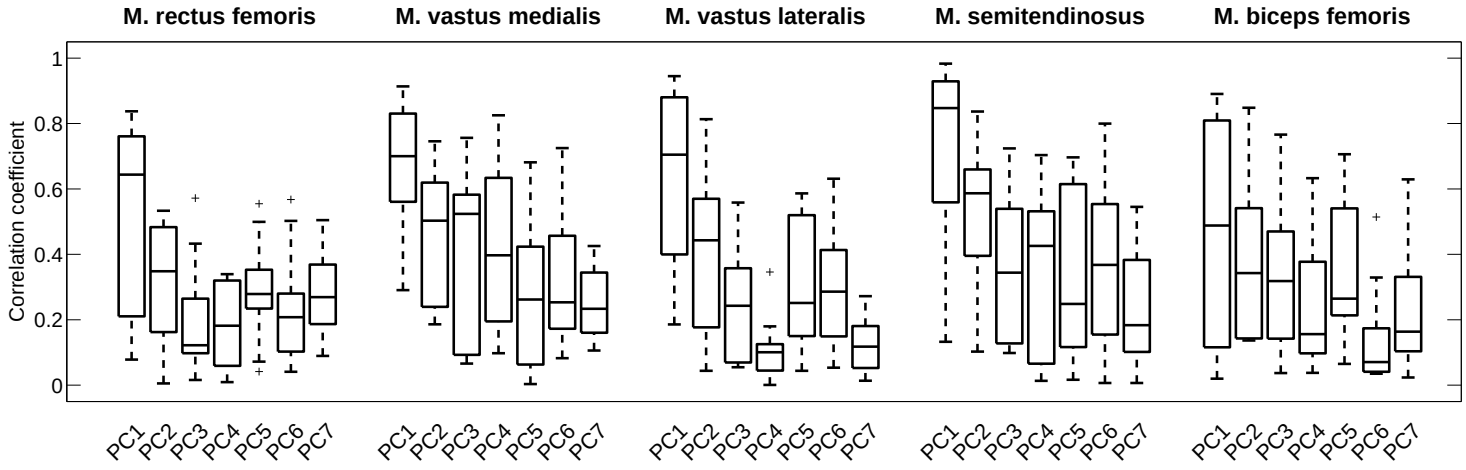
M. rectus femoris
M. vastus medialis
M. vastus lateralis
M. semitendinosus
M. biceps femoris
Correlation coefficient
0
0.2
0.4
0.6
0.8
1
PC1
PC2
PC3
PC4
PC5
PC6
PC7

Fig#5

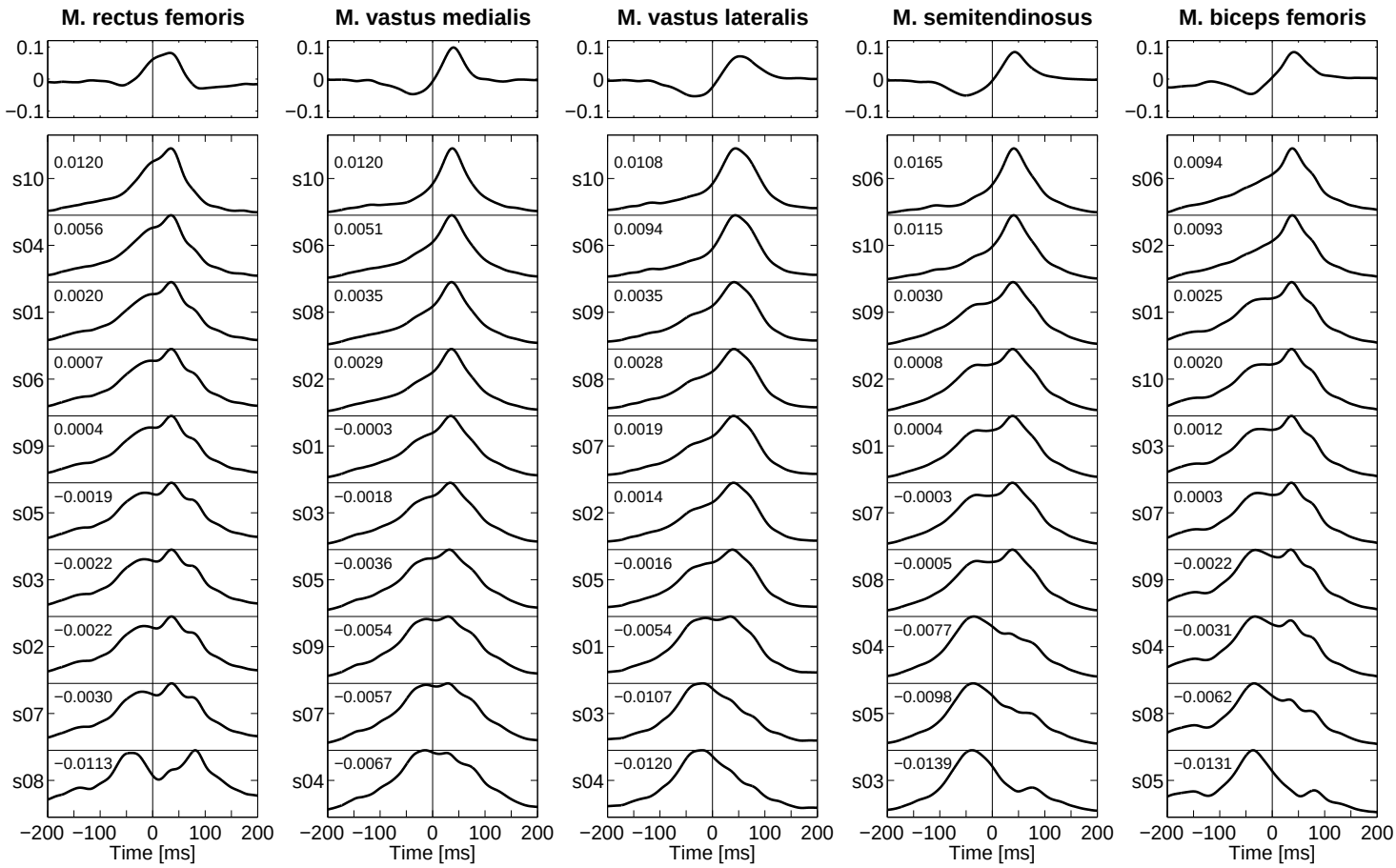
M. rectus femoris
M. vastus medialis
M. vastus lateralis
M. semitendinosus
M. biceps femoris
0.1
0
−0.1
s10 0.0120
s04 0.0056
s01 0.0020
s06 0.0007
s09 0.0004
s05 −0.0019
s03 −0.0022
s02 −0.0022
s07 −0.0030
s08 −0.0113
s10 0.0120
s06 0.0051
s08 0.0035
s02 0.0029
s01 −0.0003
s03 −0.0018
s05 −0.0036
s09 −0.0054
s07 −0.0057
s04 −0.0067
s10 0.0108
s06 0.0094
s09 0.0035
s08 0.0028
s07 0.0019
s02 0.0014
s05 −0.0016
s01 −0.0054
s03 −0.0107
s04 −0.0120
s06 0.0165
s10 0.0115
s09 0.0030
s02 0.0008
s01 0.0004
s07 −0.0003
s08 −0.0005
s04 −0.0077
s05 −0.0098
s03 −0.0139
s06 0.0094
s02 0.0093
s01 0.0025
s10 0.0020
s03 0.0012
s07 0.0003
s09 −0.0022
s04 −0.0031
s08 −0.0062
s05 −0.0131
−200 −100 0 100 200
Time [ms]

Fig#6

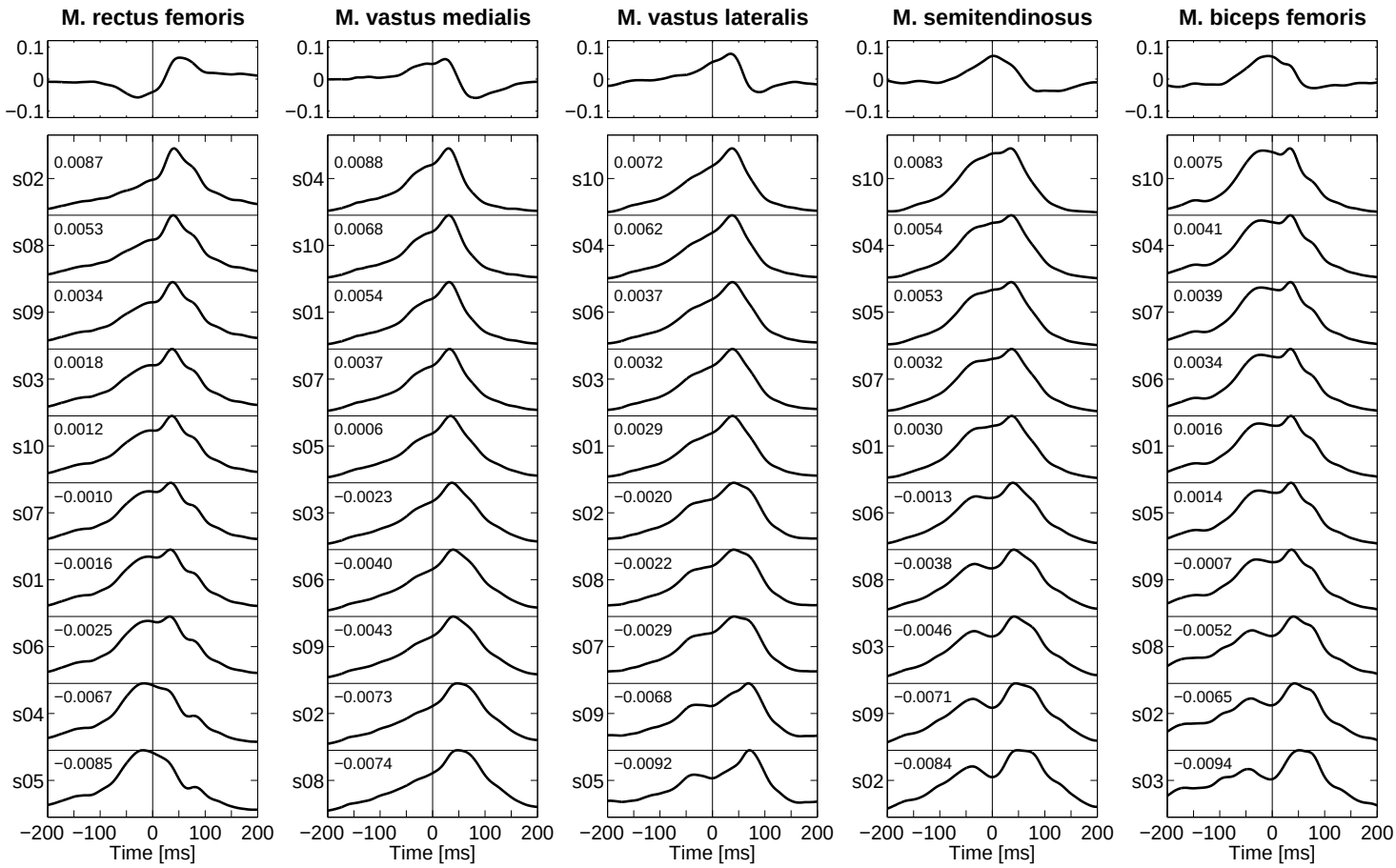
M. rectus femoris
M. vastus medialis
M. vastus lateralis
M. semitendinosus
M. biceps femoris
0.1
0
−0.1
s02 0.0087
s08 0.0053
s09 0.0034
s03 0.0018
s10 0.0012
s07 −0.0010
s01 −0.0016
s06 −0.0025
s04 −0.0067
s05 −0.0085
s04 0.0088
s10 0.0068
s01 0.0054
s07 0.0037
s05 0.0006
s03 −0.0023
s06 −0.0040
s09 −0.0043
s02 −0.0073
s08 −0.0074
s10 0.0072
s04 0.0062
s06 0.0037
s03 0.0032
s01 0.0029
s02 −0.0020
s08 −0.0022
s07 −0.0029
s09 −0.0068
s05 −0.0092
s10 0.0083
s04 0.0054
s05 0.0053
s07 0.0032
s01 0.0030
s06 −0.0013
s08 −0.0038
s03 −0.0046
s09 −0.0071
s02 −0.0084
s10 0.0075
s04 0.0041
s07 0.0039
s06 0.0034
s01 0.0016
s05 0.0014
s09 −0.0007
s08 −0.0052
s02 −0.0065
s03 −0.0094
−200 −100 0 100 200
Time [ms]

Fig#7

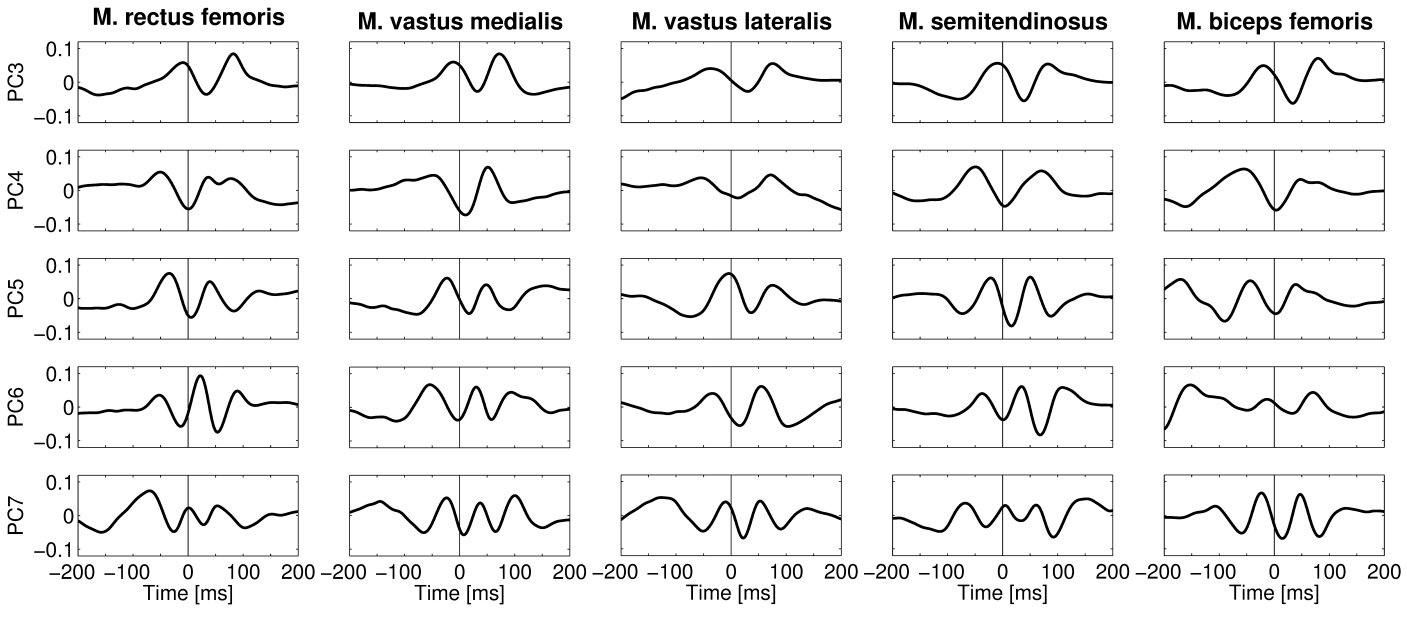
M. rectus femoris
M. vastus medialis
M. vastus lateralis
M. semitendinosus
M. biceps femoris
PC3
PC4
PC5
PC6
PC7
0.1
0
−0.1
−200 −100 0 100 200
Time [ms]